EMPIRICAL MODELLING AND EXPERIMENTAL INVESTIGATION ON ABSORPTION SPECTRA OF COLLOIDAL METAL NANOPARTICLES AND QUANTUM DOTS SUSPENDED IN IONIC SURROUNDING MEDIA

by

BAHARAK MEHRDEL

Thesis submitted in fulfilment of the requirements
for the Degree of
Doctor of Philosophy

April 2019

ACKNOWLEDGEMENT

First of all, I would like to express my sincere thanks to my main supervisor, Professor Dr. Azlan Abdul Aziz for his encouragement, patience, trust and invaluable advices and guidance in this work. I have benefited a lot of things from him which cover both non-technical and technical skills. The second person who I would like to express my thanks and appreciation to my co-supervisor Assoc. Prof. Dr. Yoon Tiem Leong for his complementary recommendations and guidance to this work. I would like to thank is my co-supervisor Dr. Nurulhasanah Binti Othman. Her expertise and experience in the field of mass spectroscopy and proteomics are really helpful to the quality of research. Without their professional guidance and continuous supports, this research work would be an impossible task to me.

I am indebted to all technical staffs in the Institute for research in molecular medicine (INFORMM) and the School of Physics for their kind assistance in experimental works. Besides, I would like to express my appreciation to Dr. Lee Sai Cheong, Dr. Ashwaq Hamid Salem Yehya, Shandra Devi, Siti Nur Shafiqa, Mahmood Subri Jameel and Mohammed Ali Dheyab, Gaayathri Kumarasamy and Jorim Anak Ujang for their help and support during my study.

Last, but never the least, I would like to thank my family for encouraging me to complete the study and greatest support all the time.

TABLE OF CONTENT

ACKNOWLEDGEMENT ii

TABLE OF CONTENT iii

LIST OF TABLES vii

LIST OF FIGURES ix

LIST OF SYMBOLS xiv

LIST OF ABBREVIATIONS xv

ABSTRAK xvi

ABSTRACT xviii

CHAPTER 1 - INTRODUCTION

1.1 Motivation 1

1.2 Research gap 4

1.3 Problem statement 6

1.4 Objectives of work 7

1.5 Scope of work 7

1.6 Contribution of the dissertation 8

1.7 Organization of the dissertation 9

CHAPTER 2 - LITERATURE REVIEW

2.1 Introduction 10

2.2 Theoretical modelling of surface plasmon resonance of nanoparticles 11

2.2.1 Mie theory 11

2.2.2 General assumption of effective medium theory 12

2.3 Factors influencing surface plasmon resonance 13

2.3.1 Chemical-physical properties of environment 13

2.3.2 Plasmon resonance sensitivity with a refractive index of surrounding media and nanoparticle size 15

2.3.3 Effect of ionic media on nanoparticle colloidal 17

2.4 CdSe/ZnS Quantum dots 19

2.5 CdSe/ZnS Quantum dots as ion sensing of local surrounding media 23

2.6 Overview of research on cavity models 24

2.7 Chapter summary 25

CHAPTER 3 - THEORETICAL BACKGROUND

3.1 Introduction 26

3.2 Colloidal solutions 26

3.2.1 Polydispersity 26

3.3 Chemical interface damping 27

3.4 Theoretical background 28

3.4.1 Radiative properties of noble metal nanoparticles 28

3.4.2 Lorentz-Drude size-dependent dielectric function models 32

3.4.3 Effective medium theory approach 34

3.4.4 Correlation between refractive index and concentration 35

3.4.5 Complex dielectric function by Kramer-Kronig in optical materials ... 36

3.5 Semiconductor nanoparticles 37

3.5.1 Radiative properties of CdSe/ZnS Quantum dots 39

3.5.2 Dependence of absorption on the surrounding media refractive index 40

3.6 Chapter summary 45

CHAPTER 4 - MATERIAL AND METHODOLOGY

4.1 Introduction 46

4.2 Materials 48

4.3 Experimental tools 49

4.3.1 TEM measurement 49
4.3.2 Zetasizer measurements 50
4.3.2(a) Dynamic light scattering (DLS) 50
4.3.2(b) Zeta potential 52
4.3.3 UV-VIS-NIR Spectrophotometer 54
4.3.4 Fluorescence spectrophotometer 55
4.3.5 Refractometer 55
4.4 Experimental methods 55
4.4.1 Media preparation: NaCl, NaOH, PBS 58
4.4.1(a) NaCl stock solution 58
4.4.1(b) NaOH stock solution 58
4.4.2 AuNPs and AgNPs preparation 59
4.4.3 Quantum dots preparation 59
4.4.4 Sample preparation for the experiment 60
4.5 Software implementation 61
4.6 Sensitivity calculation of spectra 65
4.7 Chapter summary 66

CHAPTER 5 - PLASMON RESONANCE SENSITIVITY OF METAL NANOPARTICLE: SIZE AND IONIC MEDIA IDENTITY

5.1 Introduction 67
5.2 Geometry and size distribution characterization of metal nanoparticles 67
5.3 Refractive index calculation of media 70
5.4 Size-dependent and effective dielectric function of metal nanoparticles 73
5.5 Effect of calculated plasmon resonance sensitivity on the size and the refractive index of non-absorbent ionic media 88
5.5.1 Calculated plasmon resonance sensitivity for AuNPs 88
5.5.2 Calculated plasmon resonance sensitivity for AgNPs 90

5.6 Comparison between calculated and empirical plasmon resonance sensitivity 93

5.6.1 Size and electrolyte dependent of plasmon resonance sensitivity of AuNPs 94

5.6.2 Size and electrolyte dependent of plasmon resonance sensitivity of AgNPs 110

5.7 Chapter summary 121

CHAPTER 6 - ABSORPTION CROSS SECTION OF QUANTUM DOTS DEPENDENCE ON: SIZE AND IONIC MEDIA IDENTITY

6.1 Introduction 122

6.2 Geometry and size characteristic of quantum dots suspension 122

6.3 Effect of concentration and background electrolyte on the zeta potential and hydrodynamic size 125

6.4 Effect of the background electrolyte refractive index on the photophysical properties 130

6.5 Chapter summary 139

CHAPTER 7 - CONCLUSIONS AND FUTURE STUDIES

6.6 Conclusions 141

6.7 Future studies 142

REFERENCES 144

APPENDICES

LIST OF PUBLICATIONS

LIST OF TABLES

Page

Table 1.1 Studies of influence of media on noble metal nanoparticles and semiconductor Qdots. 6

Table 4.1 Samples information and properties are given by the manufacturer 48

Table 4.2 The list of general chemicals used in this study. 58

Table 4.3 Salt concentration preparation for NaCl, NaOH and PBS. 59

Table 5.1 Properties of metal nanoparticles measured: TEM, DLS and FWHM of absorption spectra. 70

Table 5.2 Refractive index for different concentration of NaCl and NaOH solutions with different methods and refractometer measurement.
The |δRI| is the absolute value of (RI calculated – RI measured) refractive index. The absolute value was used due the negative value in the case of 0.15M and 1M. Measured at wavelength 520 nm. 72

Table 5.3 SPSS results. The significance level is greater than 0.05 the variances between three groups are equal. The value is greater than 0.05, the difference is not statistically significant. 73

Table 5.4 The dips at real epsilon and maximum peak of real and imaginary part of epsilon in two concentration of NaCl (0.01M and 1M). 80

Table 5.5 The variation in volume fraction will affect the plasmon resonance position. 83

Table 5.6 Effect of NaCl on the zeta potential, hydrodynamic diameter (HDD), absorption width (FWHM) and area under plasmon resonance of AuNPs. In the case of 20 and 80 nm AuNPs, the FWHM in specific threshold salt concentration has two values, plasmon resonance in lower wavelength and coupling plasmon resonance in higher wavelength. 100

Table 5.7 Effect of types of electrolyte on the hydrodynamic diameter (HDD) and SPR of AgNPs. (a) 20 nm, (b) 50 nm, (c) 80 nm silver suspended in sodium citrate. 112

Table 6.1 The properties of the primary Qdots nanocrystal, TEM and DLS results of measurement in water as a media. 124

Table 6.2 Comparison of the three models against the empirical log-log slope in NaCl aqueous medium. 135

Table 6.3 Comparison of the three models against the empirical log-log slope in NaOH and PBS medium. 138

LIST OF FIGURES

Page

Figure 1.1 General mechanism of stimulated and spontaneous emission. 3

Figure 3.1 Surface plasmon resonance oscillation of noble metal nanoparticle electrons, effecting of the strong increase of the electric field. 31

Figure 3.2 The scheme is adopted from Issam et al., presents energy bandgap structure of CdSe/ZnS [134]. 38

Figure 3.3 Measured broad absorption spectra and narrow photoluminescence (emission) band of semiconductor quantum dots (CdSe/ ZnS) 39

Figure 3.4 Left: Water-soluble CdSe/ZnS colloidal quantum coated with carboxyl acid. Right: Hypothetical (virtual) spherical cavity (shown as dotted sphere). In the VC model, the cavity is filled with medium, while in the EC model medium is expelled from occupying the cavity. Core- centred dipole is shown as the green double arrow. In the case of the EEC model, the virtual boundary of the cavity becomes ellipsoid. 41

Figure 3.5 A general ellipsoidal cavity model with an electronic transition dipole moment μ. 44

Figure 4.1 General flowchart of theoretical and experimental design used in this study 47

Figure 4.2 Plots of size distribution of (a) small particle and (b) large particle (aggregated particle) based on light scattered by particles. The plots adopted from Malvern panalytical company [156]. 51

Figure 4.3 Electric double layer surrounding NPs. The scheme adopted from Malvern panalytical company [158]. 53

Figure 4.4 Zeta Potential predicts stability. The scheme adopted from Horiba website [159]. 54

Figure 4.5 Flowchart of the procedure for experimental measurement and data analysis of optical absorption spectra to surrounding media for NPs. 57

Figure 4.6 Sample preparation of NPs and ionic media. (1) preparation of different salt solution, (2) adding NPs colloids suspension, (3) instant analysis of samples by optical absorption and DLS measurements. 61

Figure 4.7 Flowchart of theoretical modelling of the sensitivity of optical absorption spectra to surrounding media for NPs. 63

Figure 4.8 Flowchart of fitting best model on experimental data of Qdots in different surrounding media. 64

Figure 4.9 First derivative absorption spectra from the measured absorption spectra in different NaCl concentrations. 66

Figure 5.1 Size distribution histogram of (a) 10 nm, (b) 20 nm and (c) 80 nm AuNPs. TEM images indicate the physical structure of AuNPs used in this work. 68

Figure 5.2 Size distribution histogram of (a) 20 nm, (b) 50 nm and (c) 80 nm AgNPs. TEM image indicates the physical structure of AgNPs used in this work. 69

Figure 5.3 Measured RI as a function of non-absorbent ionic media concentration 71

Figure 5.4 (a) Real part (n) and (b) imaginary part (k) of refractive indices of AuNPs in different size by Lorentz-Drude; (c) Mie extinction spectra shows the effect of size depended dielectric function in water with refractive index nm = 1.3. 75

Figure 5.5 Calculated real and imaginary parts of the refractive index by using the effective medium theory and Eq. (3.11). (a) real and (b) imaginary part for 0.01M NaCl. 78

Figure 5.6 Calculated real and imaginary parts of the refractive index by using the effective medium theory and Eq. (3.11). (a) real and (b) imaginary part for 1M NaCl. 79

Figure 5.7 Experimental absorption in different volume fractions of 10 nm gold nanoparticles in 0.01M (a) and 1M (b) NaCl. In both figures the primary plasmon resonance of 10 nm gold are shown. The impact of the CID effect on lowering and broadening of plasmon resonance clearly appear in experimental data. The hydrodynamic size (nm) of aggregated gold nanoparticles is shown inside the parenthesis. 82

Figure 5.8 The size distribution of 30% of 10nm gold by using the dynamic light scattering. (a) 0.01M NaCl (b) 1M NaCl. 84

Figure 5.9 The aggregation of AuNPs, the color of the solution is changed from red to violet. 84

Figure 5.10 The hydrodynamic size of AuNPs versus volume fraction of two salt concentrations (0.01M and 1M NaCl). 85

Figure 5.11 Real and imaginary part of the refractive index calculated from experimental absorption spectra by Kramer-Kronig simulation. 86

Figure 5.12 Comparison of red shift of real part (n) and imaginary part (k) of the refractive index for different volume fraction of 10 nm AuNPs in 1 M and 0.01 M NaCl solutions. 87

Figure 5.13 Mie scattering theory calculated for AuNPS as a function of salt concentration (surrounding media assumed to be wavelength depended (n_NaCl (λ)). (a) particle size vs. maximum value of absorption. (b) particle size vs. surface plasmon resonance. 89

Figure 5.14 The variation of calculated S_Mie as a function of particle size. 90

Figure 5.15 Mie scattering theory calculated for AgNPS as a function of salt concentration (surrounding media assumed to be wavelength depended (n_NaCl (λ)). (a) particle size vs. maximum value of absorption. (b) particle size vs. surface plasmon resonance. 92

Figure 5.16 The change of Mie scattering theory sensitivity of damping (nm -1) vs. particle size (nm). 93

Figure 5.17 (i) Calculated SPR wavelength and (ii) experiment SPR wavelength of three AuNPs as a function of NaCl concentration and the maximum magnitude of absorption spectra. (a) 10 nm, (b) 20 nm, and (c) 80 nm. SPR wavelength not predicted by Mie scattering theory due to calculate single AuNPs. In experiment, however, aggregation happens and coupling plasmon resonance observes. 96

Figure 5.18 Calculated (Mie) maximum SPR vs. refractive index of NaCl (measured). The sensitivity of refractive index calculated for 10 nm is 260 and in the case of 20 and 80 nm are 280 and 270 nm/RIU respectively. 97

Figure 5.19 The relation between particle size and (a) Maximum plasmon resonance, (b) coupling plasmon resonance shift in different salt concentration. 99

Figure 5.20 First derivative absorption spectra from the measured absorption spectra in different NaCl concentrations. 103

Figure 5.21 Calculated S_Mie and S_exp for 3 different AuNPs size are compared. The left-side plots show the sensitivity as a function of NaCl concentration. The right-side plots show the close look at concentrations less than threshold concentration (b) 10 nm AuNPs at concentrations less than 0.1M, (d) 20 nm AuNPs at concentrations less than 0.04 M, (f) 80 nm AuNPs at concentrations less than 0.03 M. 106

Figure 5.22 Comparing between NaOH and PBs for SPR sensitivity of damping (S_exp) for AuNPs (10, 20, 80 nm). 108

Figure 5.23 Comparison of the S_exp between NaCl, NaOH, PBS vs particle size at threshold concentration for each AuNPs size. 109

Figure 5.24 Calculated and empirical sensitivity of SPR damping for three different AgNPs size (20, 50 and 80 nm). 115

Figure 5.25 The left-hand side shows comparison between NaCl and NaOH solutions for SPR sensitivity of damping for AgNPs and the right-hand side shows the zoom at low concentration. (a) and (b) 20 nm, (c) and (d) 50 nm, and (e) and (f) 80 nm. 117

Figure 5.26 The zoom of SPR sensitivity of damping for AgNPs at low concentration. (a) 20 nm, (b) 50 nm, and (c) 80 nm. 118

Figure 5.27 Comparison between sensitivity of damping (S_exp (nm-1)) for NaCl, NaOH and PBS (0.04M) vs particle size (nm). 120

Figure 6.1 TEM image of CdSe/ZnS colloidal quantum dots (a) QD 550 (Green), (b) QD 620 (Red), and (c)QD 640 (Dark Red). 123

Figure 6.2 Emission spectra of primary water soluble CdSe/ZnS core-shell colloidal quantum dots. (Green Qdots emitting at 550 nm, red Qdots emitting at 620 nm, Dark red Qdots emitting at 640 nm). 125

Figure 6.3 The effect of concentration on the measured zeta potential and hydrodynamic diameter (A) Green (QD 550), (B) red (QD 620) and (C) dark red (QD 640). The error bars (standard deviation) were derived from the measured data. In some cases, the error bars at some data points are not vividly visible due to its overly suppressed magnitude. 127

Figure 6.4 The log-log slope of the EC model is presented by broken line. Dotted line curve represents the log-log slope of the VC model. The log-log slope of the EEC model is presented by solid lines. Note that the slope of the EEC model is the same as that of the empirical slope, x (shown as colored dashed lines labelled 'empirical fit') (a) green (QD 550), (b) red (QD 620) and (c) dark red (QD 640) quantum dots suspended in NaCl. The effective value $ln\,\bar{n}$ is indicated as '*'. The error bars (standard deviation) were derived from the measured data. Note that the error bars at some data points are not vividly visible due to its overly suppressed magnitude. 134

Figure 6.5 Three cavity models applied on non-absorbent ionic media with hydrogen bonding (a) and (d) Green (QD 550), (b) and (e) Red (QD 620), and (c) and (f) Dark Red (QD 640). The (a), (b) and (c) are suspended in NaOH and (d), (e) and (f) are suspended in PBS. Note that specifically in (a) the slopes in the VC and EEC models coincide with the empirical fit. The error bars (standard deviation) were derived from the measured data. 137

LIST OF SYMBOLS

σ	Absorption cross section
ε	Dielectric constant
ω	Frequency
ε_i	Imaginary part of the metal-dielectric function
ε_m	Medium dielectric constant
ε_0	Permittivity of free space
ε_r	Real part of the metal-dielectric function
η	Viscosity of the solution
λ	Wavelength
ζ	Zeta potential
n	Refractive index

LIST OF ABBREVIATIONS

AgNPs	Silver nanoparticles
AuNPs	Gold nanoparticles
CdSe/ZnS	Cadmium-selenium/zinc-sulfide
DLS	Dynamic light scattering
EC	Empty cavity
EEC	Empty ellipsoidal cavity
EM	Electromagnetic
EMT	Effective medium theory
NaCl	Sodium chloride
NaOH	Sodium hydroxide
NPs	Nanoparticles
OD	Optical density
PBS	Phosphate buffered saline
Pw	Peak width
Qdots	Quantum dots
QY	Quantum yield
RET	Resonance energy transfer
RI	Refractive index
SPR	Surface plasmon resonance
TEM	Transmission electron microscopy
UV/Vis/NIR	Ultra violet/ visible/ near infrared
VdW	Van der waals
VC	Virtual cavity
Xe	Xenon

PERMODELAN SECARA EMPIRIK DAN PENYIASATAN EKSPERIMENTAL KEATAS SPEKTRA PENYERAPAN LOGAM NANOPARTIKEL KOLOIDAL DAN TITIK KUANTUM TERAMPAI DALAM PERSEKITARAN MEDIA IONIK

ABSTRAK

Kajian ini menyiasat pengaruh saiz nanopartikel dan indeks biasan media sekitar ionik yang tidak menyerap, ke atas spektrum penyerapan optik nanopartikel logam mulia (Au, Ag; pelepasan yang teruja) dan titik kuantum semikonduktor (CdSe / ZnS; pelepasan spontan) yang direka untuk aplikasi pengesanan. Banyak kajian melalui penyelidikan secara eksperimen telah menunjukkan bahawa, spektrum penyerapan optik nanopartikel logam mulia dan semikonduktor titik kuantum sangat bergantung kepada saiz nanopartikel dan indeks biasan media sekitar, sementara kurang persandaran kepada indeks biasan media sekitar ionik yang tidak menyerap yang secara beransur-ansur berubah dari 1.33 ke 1.34. Walau bagaimanapun, masih terdapat kekurangan maklumat mengenai kesan identiti media sekitar untuk nanopartikel logam mulia dan semikonduktor titik kuantum sebagai fungsi saiz nanopartikel. Untuk menangani isu ini, kaedah terbitan pertama digunakan untuk simulasi spektrum penyerapan teori Mie dan spektrum penyerapan eksperimen nanopartikel bagi penilaian secara kuantitatif resonans spektrum. Untuk mengenal pasti pengaruh identiti media sekeliling ionik pada spektrum optik yang diukur untuk nanopartikel logam mulia dan semikonduktor titik kuantum, satu siri eksperimen dilakukan menggunakan natrium klorida (NaCl), natrium hidroksida (NaOH), dan fosfat salin bertimbal (PBS). Khususnya, teori Mie mula-mula digunakan dengan pengubahsuaian kecil kepada pemalar dielektrik nanopartikel logam (bergantung

kepada saiz Lorentz-Drude) diikuti dengan rawatan kaedah terbitan pertama untuk menganalisis spektrum penyerapan optik. Hasil daripada kaedah terbitan pertama menunjukkan secara teori, tindak balas optik mencapai sensitiviti maksimum pada jarak antara 50 hingga 60 nm dan 20 hingga 30 nm bagi AuNPs dan AgNPs, menunjukkan kebergantungan spektrum optik kepada saiz. Sebaliknya, hasil eksperimen pula menunjukkan bahawa tindak balas optik terhadap media sekitar bergantung kepada identiti media sekitar dan jenis nanopartikel logam mulia. Hal ini telah mendedahkan bahawa tindak balas optik AuNPs saiz kecil (~ 10 nm) dan AgNP yang bersaiz besar (~ 80 nm) tidak sensitif kepada identiti media sekeliling. Dalam kes semikonduktor titik kuantum, tiga model rongga dengan pernyataan penyerapan keratan rentas sebagai fungsi indeks biasan daripada medium bukan penyerap telah digunakan. Pemasangan model teori (rongga kosong elipsoid) dengan data eksperimen menunjukkan bahawa jenis dan polariti media sekeliling sangat mempengaruhi bentuk geometri model rongga kerana kehadiran atau ketiadaan ikatan hidrogen dalam media ini. Secara ringkasnya, kajian ini memberikan gambaran mengenai aplikasi penderiaan kimia berdasarkan spektrum penyerapan dengan menggunakan model empirikal baru untuk menghasilkan spektrum output dalam media sekitar yang tidak menyerap untuk nanopartikel Au, Ag dan CdSe / ZnS Qdots berdasarkan saiz nanopartikel.

EMPIRICAL MODELLING AND EXPERIMENTAL INVESTIGATION ON ABSORPTION SPECTRA OF COLLOIDAL METAL NANOPARTICLES AND QUANTUM DOTS SUSPENDED IN IONIC SURROUNDING MEDIA

ABSTRACT

This study investigates the influence of the nanoparticle size and refractive index of non-absorbent ionic surrounding media on the optical absorption spectra of noble metal nanoparticles (Au, Ag; excited emission) and semiconductor quantum dots (CdSe/ZnS; spontaneous emission) designed for sensing application. Numerous studies on experimental research have shown that, the optical absorption spectra of noble metal nanoparticles and quantum dots are strongly dependent on the nanoparticle size and refractive index of surrounding media, while weakly dependent on the refractive index of non-absorbent ionic surrounding media which gradually change from 1.33 to 1.34. However, there is still lack of information on the effect of identity of the surrounding media for noble metal nanoparticles and quantum dots as a function of particle size. To address this issue, the first derivative method was applied to simulated absorption spectra of Mie theory and experimental absorption spectra of nanoparticles to quantitatively evaluate the spectra resonance. To determine the influence of identity of ionic surrounding media on the measured optical spectra for noble metal nanoparticles and semiconductor quantum dots, a series of experiments were performed using sodium chloride (NaCl), sodium hydroxide (NaOH), and phosphate buffered saline (PBS). Specifically, the Mie theory was employed, with minor modification to the dielectric constant of metal nanoparticles (Lorentz-Drude size dependent) followed by the first derivative method treatment to analyse the optical absorption spectra. Results from the first derivative method showed the theoretical

optical response reaches the maximum sensitivity at size ranges of 50 to 60 nm and 20 to 30 nm for AuNPs and AgNPs, respectively which implies size dependent of optical spectra. On the other hand, the experimental results showed that optical response to surrounding media were dependent on the identity of surrounding media and type of noble metal nanoparticles. It was revealed that optical response of tiny AuNPs (~10 nm) and large AgNPs particles (~ 80 nm) were insensitive to the identity of surrounding media. In the case of semiconductor quantum dots, three cavity models with expression of absorption cross-section as a function of refractive index of non-adsorbent medium were employed. The fitting of the theoretical model (ellipsoidal empty cavity) with experimental data revealed that type and polarity of surrounding media strongly influence the geometrical shape of the cavity models due to the presence or absence of hydrogen bonds in these media. In summary, this study provides an insight into chemical sensing application based on absorption spectra by using the new empirical modelling for absorption spectra output in non-absorbent surrounding media for Au, Ag and CdSe/ZnS Qdots nanoparticles based on nanoparticles sizes.

CHAPTER 1

INTRODUCTION

1.1 Motivation

Noble metal nanoparticles (excited emission) exhibit remarkable optical characteristic because of their surface plasmon resonance, which is the collective coherent oscillation of the free electrons of nanoparticles in resonance with an incident electromagnetic wave. This plasmon resonance could essentially be explained as a photon that is strongly confined to the nanoscale size of the noble metal nanoparticles. The plasmon oscillation significantly enhances the electromagnetic (EM) field around the noble metal nanoparticle, which results in strong light absorption by the noble metal nanoparticles at the plasmon resonance frequency. This property of metal nanoparticles enables their applicability in medical and optical field. From Faraday's novel work on the colors from colloidal noble metal nanoparticles, interest and research in these metal particles has evolved from empirical and artistic to scientific nanotechnology [1]. Several researches have related the shape, composition, size and surrounding environment of noble metal nanoparticles to plasmon resonance frequency as well as plasmonic damping and enhancement.

The semiconductor nanoparticles with spontaneous emission (mostly from CdSe-based material) are currently being applied in the fields of inorganic biosensing and biophotonics because of their long lifetimes, broad absorption and narrow emission band properties. The stability of semiconductor nanoparticles can be improved by coating the core (e.g. CdSe) with a higher band gap material (ZnS) [2]. The relation between the size of semiconductor nanoparticles and their electronic band gap was introduced by Luis Brus for sphere particle model approximation of the bulk

Wannier Hamiltonian. In general, the energy of the longest wavelength absorption is defined as the band gap of a semiconductor material. Based on this approximation, the size of particle (r^2) decreases with increase in band gap [3]. When the dimensions of the particle become sufficiently small, the electronic conduction band will fragment into discrete states. This effect is referred to as the quantum size effect. These discrete eigenstates are not directly observable in optical experiments of noble metal nanoparticles; however, they are present in semiconductor quantum dots (broad absorption spectra). Like semiconductor Qdots, noble metal nanoparticles display highly size dependent optical resonance, a phenomenon known as surface plasmon resonance. This plasmon oscillation is a known feature of noble metal nanoparticles because of the collective oscillations of conduction band electrons.

The Au and Ag nanoparticles (NPs) have attracted interest due to their associated surface plasmon resonance. These NPs are interested due to 1) their air stability, 2) d-d band transitions and the plasmon frequency lies in the visible region of spectrum, 3) at the plasmon frequency the imaginary part of dielectric constant is very small, and this why the near field effect is high that makes the plasmon excitation very interesting. The optimum dimension of nanoparticles is usually in the range of 0.2 to 100 nm [3]. In this nanoscale range, the surface to volume ratios of particles increase and their electronic energy state become discrete, which results in unique electronic and optical properties of the nanoparticles. Generally, as the size of metal and semiconductor particles reduces towards the nanoscale, their electronic and optical properties become size dependent. These size dependent properties of nanoparticles are attributed to the quantum confinement effect. For instance, when the spherical radius of nanoparticles is lower than the exciton Bohr radius of the nanoparticle, the strong confinement of electrons and holes will occur. Nanomaterials, such as,

CdSe/ZnS quantum dots (Qdots), gold (Au) and silver (Ag) nanoparticles have attracted considerable interest for several applications in optical devices, bioimaging, biosensing and chemical sensing because of their size dependent (tunable) optical spectra and plasmon color. Therefore, the plasmon resonance is a key factor of nanoparticles that makes them applicable for optical sensing along with their absorption line shape of spectra (Figure 1.1).

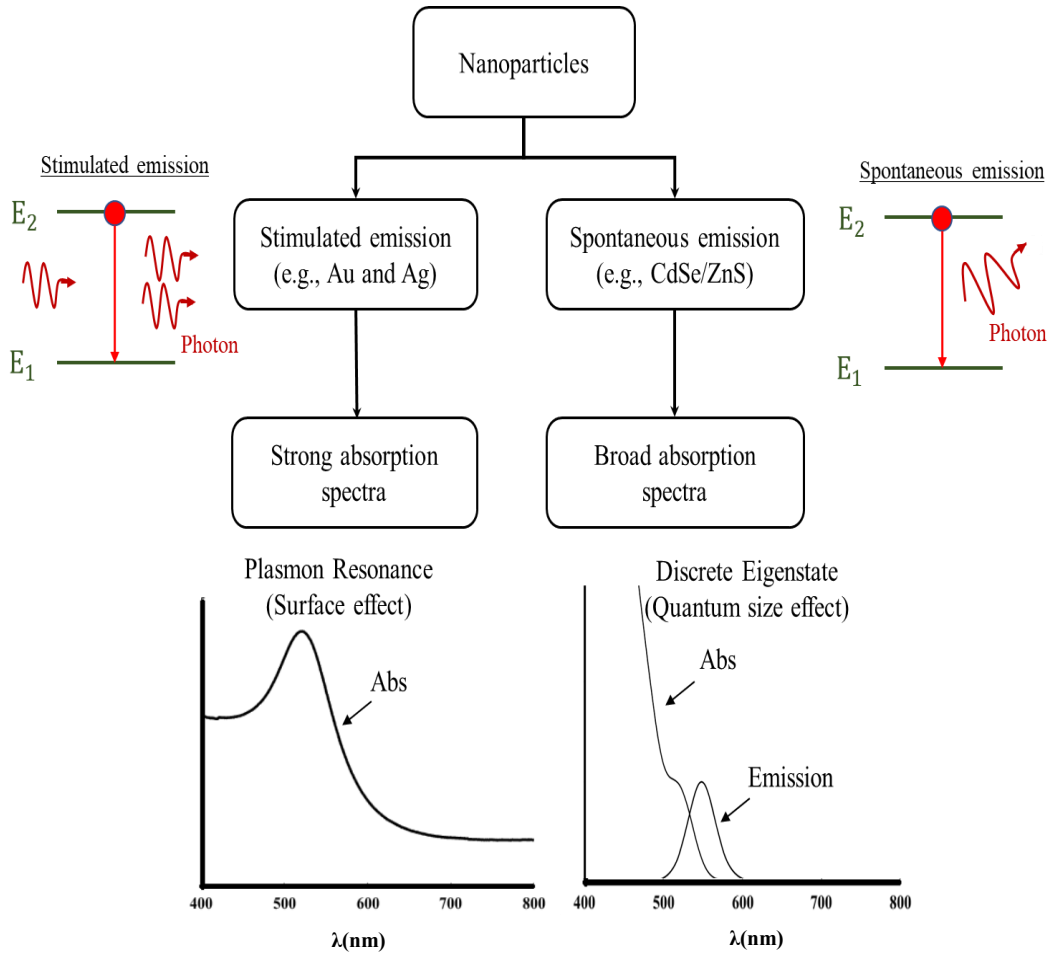


Figure 1.1: General mechanism of stimulated and spontaneous emission.

Mie theory is a general solution to Maxwell's equations for the scattering of electromagnetic radiation by any homogeneous spherical particle. Mie's theory was initially intended to describe the different dyes of colloidal noble metal nanoparticles

and their size dependence. The Mie theory confined a plane wave scattering by an isotropic and homogeneous sphere particle in a non-absorbing surrounding medium. The Mie's solution involves the application of electromagnetic (EM) waves on the surface of a spherical nanoparticle (which is submerged into a non-absorbent surrounding medium) of different orders from the lowest dipolar to higher order multipoles, depending on the size of nanoparticles relative to the wavelength of light (size parameter) [4]. However, for noble metal nanoparticles with size less than skin depth (range 20-30 nm) [5], the incident EM wave interactions or oscillations are mainly a surface phenomenon, and not bulk as in larger sizes. It can be observed from this that the optical properties of very small noble metal nanoparticles undergo size effect and the particles form polarizable medium. Therefore, quantum size effects and size are distinct features of metal nanoparticles. As the nanoparticle size becomes smaller than the mean free path, the collisions of the conduction electrons with the nanoparticle become more important and will provide additional scattering process, which is called the free path effect. This additional nanoparticle surface scattering is proportional to $1/r$ (therefore γ_{bulk} in Drude susceptibility will replaced by $(A\nu_F)/r$). This reflects the ratio of surface scattering probability, which is proportional to the surface area ($4\pi r^2$) and the number of electrons, which is proportional to the volume ($4\pi r^3/3$) [4].

1.2 Research gap

Despite the several studies on dielectric constant of surfactant coated AuNPs, there remains limited information on the influence of an isotropic ionic liquid media (i.e., NaCl liquid) and the effect of chemical interface damping (CID) on the dielectric constant of bare AuNPs [6]. The focus of previous studies has been on the effect of

ionic media on the hydrodynamic size and absorption spectra of the metal nanoparticles [4]. Nonetheless, the effect of hydrodynamic size on the refractive index of metal nanoparticles has not been fully elucidated.

Although studies have shown that the physico-chemical properties of colloidal noble metal NPs in an ionic media suspension are influenced by factors such as the surface charge of the NPs [7-9], the dependency of SPR sensitivity on the identity of surrounding ionic media in relation to size of the metal NPs remains to be understood. Moreover, the phenomenon of weakening repulsive electrostatic force in the NPs as the strength of the ionic media exceeds the threshold salt concentration has not been unravelled [4, 10].

Furthermore, regardless of the significant interest given to the impact of refractive index of the surrounding media on Qdots [11], there is dearth of information on the effect of ionic media polarity and identity of anions inside the surrounding media on the absorption cross section of CdSe/ZnS Qdots, taking into consideration the primary nanoparticle size effect.

Suspensions of noble metal nanoparticles (Au and AgNPs) and semiconductor Qdots (CdSe/ZnS) in ionic and non-ionic media have been studied (Table 1.1) to determine the influence of media on absorption and radiative decay rate of nanoparticles.

Table 1.1: Studies of the influence of media on noble metal nanoparticles and semiconductor Qdots.

Metal NPs	Local media	Method	Finding	Ref.
core shell metal NPs	Hydrocarbons, host medium (model) refractive index was varied between 1.0 and 4.0.	Modeled using Mie scattering theory.	Refractive index depends on volume fraction of NPs. AuNPs can behave as tunable refractive index material at the visible and near-infrared	[6]
gold nanowires	Host matrix of refractive index (n = 1.5)	FDTD method	Refractive index sensitivity of metal NPs is independent of NPs shape. depends on SPR location and refractive index of surrounding environment	[12]
Water-soluble CdSe/ZnS coated with carboxylic acid	Water (n = 1.33) Sucrose (n = 1.46)	Virtual Cavity	Radiative Decay Rate	[11]
CdTe with thioglycolic acid (TGA) and mercaptopropionic acid (MPA)	Water (n = 1.333) NaCl (n = 1.544)	Cavity Models	Radiative Decay Rate	[13]

1.3 Problem statement

Although particle size and refractive index of media surrounding nanoparticles and quantum dots strongly influence their optical absorption spectra, the optical absorption spectra of non-absorbent ionic surrounding media are weakly dependent on refractive index. However, there is lack of information on the influence of these non-absorbent ionic liquid media on dielectric constant and optical absorption spectra of noble metal NPs and Qdots as a function of particle size. In addition, there is lack of available information on the effect of identity of anions inside the media surrounding

the noble metal NPs and Qdots as well as their nanoparticle size on optical absorption spectra.

1.4 Objectives of work

The main objectives of this dissertation are summarized in the points below:

1. To develop an empirical modelling and improved version of existing empirical model to better describe the optical response to non-absorbing ionic surrounding media refractive index through a MATLAB code.
2. To investigate the influence of identity of the ionic surrounding media on the measured optical spectra using a series of experiments that employ sodium chloride (NaCl), sodium hydroxide (NaOH), followed by phosphate buffered saline (PBS).
3. To describe the role of the type of nanoparticles (noble metal nanoparticles and semiconductor quantum dots) in optical spectra response.
4. To investigate the primary size effects of nanoparticles on optical spectra response.

1.5 Scope of work

This dissertation investigates the optical spectra response to the non-absorbing ionic media surrounding noble metal (excited emission) and semiconductor (spontaneous emission) nanoparticles. To achieve the research objectives, this work first explains the need to study the size effect of nanoparticles. This study also attempts to resolve ways to determine if the nanoparticles can sense their surrounding media before aggregation. Therefore, attention was given to the size effects of noble metal

nanoparticle on the linewidth, damping and broadening of optical plasmon resonance in different ionic media concentrations (0.01 M to 1 M). This dissertation developed a systematic method to help to explain the size effect of nanoparticles on optical resonance damping. However, the experimental and theoretical optical spectra are not observable in noble metal nanoparticles because of their small dimensions (less than skin depth), in contrast to semiconductor Qdots that show broad optical absorption spectra. Therefore, first derivative method, which is based on Mie theory, will not be applicable in the case of noble metal nanoparticles. Instead, the small NPs require the 'cavity models' theory to investigate the optical response to the refractive index of their surrounding media. This work focuses on the correlation between refractive index and concentration of ionic media, and the sensitivity of optical spectra as a function of particle size. This work is imperative because non-absorbing ionic media will strongly affect the surface charge of nanoparticles which causes instability of nanoparticles in addition to damping and broadening of optical spectra.

1.6 Contribution of the dissertation

This dissertation contributes to the subject of empirical modelling of absorption spectra for colloidal suspensions of noble metal nanoparticles (AuNPs and AgNPs) in non-absorbent ionic surrounding media with gradual change in refractive index from 1.33 to 1.34. This empirical model is based on a numerical differential of absorption spectra with respect to the wavelength ($\frac{dAbs}{d\lambda}$).

This study also contributes to the subject of sensing ability of colloidal Qdots in surrounding media comprising hydrogen ions, based on an ellipsoidal cavity model as an expression of absorption cross section.

1.7 Organization of the dissertation

After a concise introduction in Chapter 1, various numerical and analytical methods for modelling the absorption spectroscopy for metal nanoparticles and quantum dots, as well as history of research on the effect of refractive index of surrounding media on nanoparticles and quantum dots will be reviewed in Chapter 2. The beginning sections of Chapter 3 provide the primary definitions of colloidal solution and the effect of surrounding environment, followed by theoretical background and methods for calculating and simulating optical spectra and the refractive index effect of environment on metal NPs and Qdots. Chapter 4 presents the details of samples (metal and semiconductor nanoparticles), measurements employed in this work, software implementation and calculation methods for sensitivity of spectra damping. Chapter 5 and 6 describe the results of the research. For ease of understanding and discussion, the early sections of Chapter 5 present the theoretically calculated sensitivity of optical spectra for metal NPs. After that, the calculated results were compared with experimentally derived results of sensitivity of optical spectra damping of metal nanoparticles. In Chapter 6, the calculated and experimental results of Qdots semiconductor will be compared and the best fit model will be discussed. Finally, Chapter 7 summarizes the important findings and drawbacks of suggested model for calculating the sensitivity of damping. A few suggestions for future work are also provided in this concluding Chapter.

CHAPTER 2

LITERATURE REVIEW

2.1 Introduction

The dispersion of noble metal nanoparticles (NPs) in an appropriate surrounding medium can contribute to the emergence of a prominent resonance feature in their visible optical absorption spectrum, which is referred to as surface plasmon resonance (SPR). Generally, SPR is a derivative of the coupling of photons to the collective oscillation mode of conduction electrons of metal NPs [4, 14]. The optical properties of metal NPs are strongly dependent on the particle size, shape, coating, and local dielectric properties of surrounding media [12, 15-17]. The optical SPR sensitivity (S) of metal NPs is the key behavior that determines the potential of NPs; however, it is dependent on the chemical and physical properties of the surrounding environment of colloidal NPs. Several studies have analyzed the effect of surrounding medium refractive index on the SPR response of metal NPs [12, 17]. Nonetheless, there is lack of available information on the concentration effect (refractive index sensitivity) of non-adsorbent ionic aqueous media (e.g. NaCl and NaOH) on the optical absorption spectra of NPs (taking into consideration their size), despite the concern of environmental impact.

Therefore, this dissertation emphasizes on the refractive index sensitivity of SPR for the colloidal Au NPs and Ag NPs and absorption cross section of water-soluble CdSe/ZnS quantum dots suspended in non-adsorbent ionic aqueous media. To exemplify the importance of this research and to simplify the discussion in the latter chapters, this chapter briefly describes the common experimental and theoretical SPR and absorption cross section dependence on surrounding medium refractive index. Afterward, background knowledge and relevant studies on SPR and absorption cross

section properties as well as their effects on the refractive index of ionic surrounding media will be reviewed.

2.2 Theoretical modelling of surface plasmon resonance of nanoparticles

2.2.1 Mie theory

The study of light absorption and scattering theory by isolating spherical obstacle of any size embedded in a non-absorbing medium, based on Maxwell's equations, was initiated by Gustav Mie in 1908 [18]. This model is based on the multipole expansion of the incident and internal (particle) electromagnetic fields. Afterwards, the boundary conditions were applied across the surface of homogeneous particle. The continuity of tangential components of magnetic and electric fields were assumed. The scattered and internal fields were subsequently defined from the extension coefficients of the incident plane wave [19, 20]. In the case of metallic NPs, an accurate solution was obtained by employing the convergence of the multipole field extension, although the convergence solution must be restricted multipole orders to provide a finite number of orders. However, there is no specific equation and formula to evaluate the number of significant coefficients [4, 21].

Later, the Mie theory was developed for a coated sphere by Aden in 1951 [22] and Güttler in 1952 [23]. The generalized Mie theory presented as the solution for the absorption and scattering of aggregated particles (interaction forces: e.g., van der Waals attraction or chemical bonds) by Trinks [24] and the numerical evaluation by Quinten et al. [4, 25, 26], which was applied to colloidal Au and AgNPs suspension [27-29]. The Mie theory was also developed for individual spherical NP in very dilute solution. However, J. C Maxwell Garnett (1904) earlier predicted the effective medium

theory for the optical absorption spectra of the metal NPs in a closely packed environment [30, 31].

2.2.2 General assumption of effective medium theory

Effective medium theory (EMT) describes the optical response properties of a composite of at least two non-mixable inhomogeneous and unevenly shaped nanocomponents, where the components are well-separated and the interaction between NPs is disregarded [4, 32, 33]. In general, if this theory can replace the inhomogeneous component with a homogeneous component of material, then the single dielectric function ε_{eff} of the medium can be described as the optical response. Therefore, the effective dielectric function of this theory is a function of surrounding media, dielectric function of NPs properties and the concentration of particles (volume fraction) in the composite. A simple approach to the effective medium theory, which considers the shape and dipole polarizability of spherical NPs, was propounded by J. C. Maxwell Garnett in 1906 [30].

The extension of EMTs has been made by different authors [34-36]. Generally, the Maxwell-Garnett and the Bruggeman equations of EMT were modified (with different approximations) to obtain more accurate dielectric functions and optical response between theory and experiment [6, 37-40]. The mathematical description of the mentioned EMT is explained in Chapter 3. Despite the wide use of EMT, there are restricting assumptions of EMT. One of these assumptions is that the real sample composition is not considered, hence EMT will fail for the case of large NPs (compared with the wavelength of light) [4, 32, 41]. The variations in dielectric constant of surrounding media of AuNPs results in concomitant variation of the real effective medium dialectic constant (ε_{eff}).

2.3 Factors influencing surface plasmon resonance

The remarkable properties of AuNPs and AgNPs is the collective behavior of their conduction electrons that gives rise to the SPR. Consequently, plasmon resonance is a field that emerged in the 1990s and has been well researched over the years [5]. After the incident light resonant frequency interacts with the oscillation frequency of the electrons at conduction band, the electric field near the NPs surface becomes significantly increased, which in turn increases the optical extinction considerably. The position and width of SPR spectrum depend on factors such as shape and size of NPs as well as the dielectric and chemical properties of NP environment. For spherical metal NPs, SPR resonances occur in the visible and NIR spectra region, which are the spectral regions of interest due to applications for SPR sensors.

2.3.1 Chemical-physical properties of environment

Apell and co-workers [42, 43] posited that the additional damping is caused by the scattering of free electron electrons at the surface of metals which are material dependent. Since the scattering properties of NPs depends on the electron density in the metal particles, the damping of optical spectra is influenced by chemisorption, [44] physisorption or chemical reactions at the surfaces of NPs. There is some experimental evidence for the influence of chemical reaction on the damping surface of AgNPs embedded various solid rare gases shown by Charle et al [45-47]. Other experimental evidence for such an influence on AgNPs made in photosensitive glass was demonstrated by Kreibig [48]. Persson [49] discussed a model for the effect of chemical interface damping (CID), which was then expanded by Zaremba and Persson in 1993 [50] to consider the influence of the molecules of the matrix environment around the surface of particles. In the Persson model, the empty lowest unoccupied

molecular orbital (LUMOs) of acceptor molecules on the surface of NPs are combined with the free electrons in the conduction band of the metal particles. If the energy difference between two levels of the donor and acceptor is small, then the coupling is stronger. Hence, the electron transfer will occur after excitation of plasmon resonance. The excited electrons will subsequently be transferred into the affinity empty acceptor levels (surrounding) and then back to origin level after residence time of 10^{-14} s. For this reason, the electrons lose coherence with the other excited electrons during the plasmon excitation. This phenomenon corresponds to a wider bandwidth of absorption spectra. There is strong experimental evidence to show the plasmon spectra broadens when the 2 nm AgNPs clusters are produced in the gas phase and deposited on a silicon dioxide substrate, after which they are embedded in SiO_2 by co deposition of SiO_2.

Kreibig and co-workers [28, 51] demonstrated that plasmon resonance bandwidth increases when the AgNPs clusters are surrounded by high volume of SiO_2 molecules. All these studies are consistent with the model proposed by Persson [49] for CID of the surface plasmon resonance. Hence, the surface plasmon resonance spectra can be proposed as a sensitive chemical sensor of the surrounding media of NPs.

The chemical effects are extremely dependent on factors such as: NP size and the type of environment of NPs. Based on the CID model, various adsorbate molecules are characterized by different LUMO localization and energy, thus coupling of adsorbate molecules with the metal conduction band results in different surface plasmon resonance widths [52].

2.3.2 Plasmon resonance sensitivity with a refractive index of surrounding media and nanoparticle size

The remarkable property of AuNPs and AgNPs is the collective behavior of their conduction electrons that gives rise to the surface plasmon resonance. Consequently, plasmonic is a field that emerged in the 1990s and is well studied [5]. The main application of surface plasmon resonance refractive index sensitivity is found in biophysics. The plasmon resonance is related to the free charges in conduction band electrons, which are separated from their ionic core and excited by an incident electromagnetic wave such as visible optical beam. The oscillations of free electrons and electromagnetic field are intrinsically linked. From the viewpoint of electrical charge, this phenomenon is referred to as a polariton, whereas it is considered a plasmon in electromagnetics. Accordingly, plasmon resonance corresponds to the coupling of mechanical fluctuation of charges with the electromagnetic fluctuation of electric field. This phenomenon at the nanoscale is depicted by different colors, for example, spherical AuNPs colloids display a red-purple color [28]. These optical properties of Au and AgNPs have garnered immense attention. The slight change in color is observed when their sizes, shapes and surrounding media are modified.

Furthermore, the surface plasmon resonance is strongly sensitive to the dielectric properties of the surrounding media of Au and AgNPs. According to literature, the strong maximum polarization is satisfied by the equation: $\varepsilon_r = -2\varepsilon_m$ [5]. Thus, an increase in the medium dielectric constant ε_m results in an increase in the negative value of the real part of dielectric, which causes a red shift in the surface plasmon resonance wavelength position. These media include the presence of adsorbates or the solvent or surface capping molecules [53-55].

The refractive index and dielectric function sensitivities of NPs are being studied since a few decades ago. Dielectric materials with low or negative refractive index have been studied theoretically and experimentally [56-58]. For instance, S. Kubo et al. (2007) studied the possibility of refractive index tunability in the visible region for colloidal, spherical and core shell metal NPs suspended in hydrocarbons. This work experimentally and theoretically explored the complex refractive index tunability of AuNPs in surrounding medium. They found that refractive index in the visible range depends on the volume fraction of AuNPs. Furthermore, they were able to demonstrate that AuNPs can behave as tunable refractive index material at the visible and near-infrared optical spectrum [6].

Early investigations of the sensitivity of the plasmon response of Au and Ag nanosphere were mostly conducted on the effect of geometrical parameters [15] and change in the refractive index of surrounding media [53]. For instance, Yugang Sun and Younan Xia (2002) comparatively analyzed the sensitivities of plasmon resonances of Au nanoshell and solid colloidal Au in different surrounding media. They found the refractive index sensitivity is 60 nm/RIU for AuNPs sized 50-60 nm in diameter in plasmon resonance wavelength of 530 nm [59]. Jack et al. (2003) reported a value of 160 nm/RIU for AgNPs (diameter 40-90 nm) embedded in oils at plasmon resonance wavelength of 435 nm [60].

Nidhi Nath and Ashutosh Chilkoti (2004) demonstrated that the surface plasmon resonance (SPR) of a chemisorbed monolayer of AuNPs on the transparent substrate is strongly influenced by particle diameter in the range of 12- 48 nm. They also discovered that the extinction of AuNPs does not increase linearly with the coverage of NPs. Their results indicated that the chemical interactions and plasmon coupling between NPs could play an important role in defining the optical properties

of immobilized NPs. The study concluded that the 39 nm diameter sized AuNP exhibited the maximum sensitivity to changes in refractive index [61].

Keyeong-Seok and Mostafa A. El-Sayed (2006) also studied the effect of size, shape and metal composition of Au and Ag NPs on plasmon sensitivity. Sensitivity was found to increases linearly with increase in nanoparticle size [14]. Li et al. (2010) designed Au nanorods based localized surface plasmon resonance sensors for the detection of small biological molecules. The sensor response was measured as the change in differential extinction at the wavelength of maximum initial differential extinction [62].

Saison-Francioso et al. (2015) have studied numerically by using the finite difference time domain (FDTD) method and they found out the refractive index sensitivity of metal NPs in homogeneous surrounding media is independent of NPs shape and mostly depends on the surface plasmon resonance spectra location, and the refractive index of surrounding environments [12].

Therefore, a key objective of this dissertation is to determine the effect of coupling plasmon resonance on refractive index sensitivity in addition to taking the effects of damping and enhancement parameters into consideration when the effect of particle size is significant.

2.3.3 Effect of ionic media on nanoparticle colloidal

The identity of the surrounding medium is a very important factor that influences plasmon resonance sensitivity [51, 63, 64]. The sensitivity of SPR to chemical environmental conditions helps to identify the binding events on the surface of AuNP colloids [65, 66]. In recent years, interest has shifted to the diluted suspensions of spherical nanoparticles plasmon resonance, which are characterized by

red to purple color reflections at 520 nm of the absorption spectra. The surface plasmon resonance oscillation in Au and AgNPs drastically changes if the individual particles are densely packed in the reaction medium or suspended in high ionic media. As a result, the addition of salt causes unstable colloidal particles and electronic and electromagnetic coupling (aggregation) of individual Ag and AuNPs, depending on the size and shape, which results in the formation of complex absorption peak. Consequently, the surface plasmon resonance of aggregated NPs is red shifted up to 300 nm and the longitudinal plasmon resonance in optical spectra is broadened [67].

Studies of the aggregation of Au and AgNPs began few decades ago (1985). Several studies have explored the extinction of light by aggregated Ag and Au NPs in aqueous suspensions with the addition of small amounts of salt solution [4, 24, 25, 68-72]. Kae sato et al. (2003) investigated the aggregation behavior of AuNPs with different concentrations of NaCl, based on the solution color and monitored by the visible spectra. They discovered that the bare NPs aggregated immediately at 0.1 M NaCl, whereas the AuNPs functionalized with DNA did not exhibit any visible change at 2.5 M of NaCl. Therefore, the NPs dispersed in NaCl solution were stabilized via surface functionalization with probe DNA [73].

Till date, the research trend of sensitivity of optical spectral response to changes in surrounding media of NPs as well as the ease of monitoring their strong absorption or scattering is directed towards the exploitation of the plasmon metal NPs for chemical and biological sensing applications. For instance, Yisha Qiao et al. (2016) experimentally investigated the changes in hydrogen ion concentration and ionic strength of surrounding media in bovine serum albumin (BSA) by applying optical spectra spectroscopy [74]. Jianji Yang et al (2015) derived a new technique for the fast prediction of optical peak broadening and shift induced by small perturbations of

plasmon resonance for various sizes and shapes and locations of the perturbing objects [75].

Despite the numerous competitive exploits made over the years to adapt the several methods for detecting different combinations of surrounding media, such as metal ions [76-78], diagnostics and medicine [79], biosensing [80] researches, there is lack of detailed investigations on the influence of the isotropic ionic liquid media (i.e., NaCl liquid), the damping effect of chemical interface on refractive index of bare AuNPs and dependency of SPR response on the identity of surrounding ionic media in relation to the size effect of AuNPs. Previous investigations have only focused on the ionic media effects on the hydrodynamic size and absorption spectra of AuNPs [81]. Moreover, there has been no detailed study on the effect of hydrodynamic size on the refractive index and dielectric properties, which is imperative since the shape and width of absorption and dielectric function in ionic environment is key to determining the spectra changes and chemical interface damping (CID). To gain an insight into the effects of identity of ionic surrounding media on optical response of colloidal NPs, there is the need for in depth investigations of optical response in different ionic media and their relevant optical behaviors with the effect of size taken into consideration.

2.4 CdSe/ZnS Quantum dots

The rapid progress in fluorescent semiconductors NPs started in 1998, particularly cadmium selenide (CdSe) [82]. The coating of CdSe core with the higher bandgap material was the best solution for chemical and photochemical stability of these particles [83]. The surface of CdSe/ZnS core/shell, a semiconductor Qdots used in this thesis, form covalent bonds with the carboxyl group. The final shell coating the

Qdots maintains their optical properties and ensures well dispersion of the Qdots in local aqueous solutions [11]. There is a significant amount of research on using the unique optical properties of CdSe based Qdots in chemical sensing [84], biomedical and biophotonics applications [85-88]. Some researchers have used Qdots for biological imaging, biomedical and biophotonics applications, for example, in vitro and in vivo imaging and diagnostic of live cells [89-92]. Considerable efforts have also been given to elucidating bioimaging studies of CdSe/ZnS, in vitro and in vivo. For instance, Chan and Nie (1998) used CdSe/ZnS in biological detection and sensing in vitro via fluorescence techniques [93]. Akerman et al (2002) studied CdSe/ZnS coated with a lung-targeting peptide for lung tumor detection by fluorescence techniques [94].

One of the most significant factors impacting the sensing of biochemical environments and ion bonds is the refractive index of the local surrounding media. To quantify the influence of the refractive index of the local dielectric environment on the fluorescence decay rate of Qdots, various cavity models have been proposed. Studies have shown that radiative decay rate depends on the refractive index and some properties of the surrounding media [11, 95-97]. For instance, Toptygin et al. (2002) considered a fluorescence molecule inside a virtually empty ellipsoidal cavity model surrounded by homogeneous dielectric media to indicate emission spectra. The study found that the fluorescence molecule is sensitive to the polarity of the media, while the radiative decay rate is sensitive to both solvent polarity and refractive index [96]. Thus, the refractive index is usually described as the main optical property of transparent homogeneous medium. Nonetheless, the effect of refractive index on optical spectra and radiative decay rate should not be misconstrued with solvatochromic effect (the spectral shifts of emission and absorption which is solvent type dependent) [98]. The refractive index effect of the host medium on radiative decay rate was first published

in 1926 by Perrin [99]. The formula for the refractive index effect is expressed in Eqs. (2.1) and (2.2),

$$\frac{1}{\tau_0} = \frac{8\pi n^2}{c^2} v_m^2 \frac{1}{N} \int \alpha(v) dv \tag{2.1}$$

$$\frac{1}{\tau_0} = \frac{8\pi n^2}{c^2} v_m^2 \frac{ln(10)}{N_A} \int \varepsilon(v) dv \tag{2.2}$$

Where $\frac{1}{\tau_0}$ indicates the radiative decay rate, c is the speed of light in vacuum, n is the surrounding media refractive index, v_m represents the mean frequency of fluorescence emission, N is the number of fluorescent molecules per unit volume, $\alpha(v)$ the absorption coefficient at frequency v, $N_A$is Avogadro's number, $ln(10)$ is the natural logarithm of 10, $\varepsilon(v)$ is the decadic molar extinction coefficient at frequency v and the integration carried out over the entire absorption band that corresponds to the lowest excited singlet electronic state. However, Eqs. (2.1) and (2.2) are not applicable in the case of fluorescent molecules with large stoke shifts. Stricker and berg derived more accurate equations for large stoke shifts in 1962 [100], as shown below Eq. (2.3).

$$\frac{1}{\tau_0} = \frac{8\pi n^2}{c^2} \langle v_f^{-3} \rangle_{Av}^{-1} \frac{ln(10)}{N_A} \int \frac{\varepsilon(v)}{v} dv \tag{2.3}$$

Where v_f is a frequency of fluorescence emission and $\langle v_f^{-3} \rangle_{Av}^{-1}$ is the precise definition of the mean value. Eq. (2.3) has been applied to achieve theoretical estimates of radiative decay rates. However, Eq. (2.3) does not represent the radiative decay rate in expression of intrinsic properties of the fluorescence molecule.

In fact, the intrinsic property of a fluorescent molecule is defined as the dielectric transition dipole moment $\boldsymbol{\mu}_{ji}$ which is responsible for molecule emission. The two indexes j, i in the dipole moment indicate the static dipole moments of nanocrystal in distinct stationary states. $\boldsymbol{\mu}_{ji}$ symbolizes transition from i (initial state)

→ *j* (final state) [101]. Unfortunately, these expressions are inapplicable in the case of fluorescent molecule in solutions. Instead of using the term $\boldsymbol{\mu}_{ji}$, the radiative decay rate of fluorescent can be obtained in terms of $\left|\boldsymbol{\mu}_{ji}\right|^2$ for a fluorescent molecule in a medium.

Given that the fluorescent molecule is in liquid host medium, different physical models have been derived for cavity including the fluorescent molecule to analyze the refractive index effect of transparent surrounding medium. For example, Lorentz presents the relationship between the local media and macroscopic field by introducing a virtual spherical cavity, which assumes the medium comprises both inside and outside the cavity. Moreover, the model assumed the same polarizability for the molecule inside the cavity and molecules of the medium [102]. Other authors applied Lorentz field theory and his assumptions to absorption [103, 104]. Shibuya in 1983 reported that polarizability of the medium inside and outside the cavity is similar, indicating the same refractive index of medium [105]. Unfortunately, this hypothesis is not reliable if the molecule inside the cavity is dissimilar with the host medium molecules, i.e., the virtual cavity model is not applicable if emission or absorption is due to foreign molecules embedded in the host medium.

Thus, P. de Vries and A. Lagendijk in 1998 reported that the virtual cavity model is only applicable if emission or absorption is due to the main molecules of medium rather than strange molecules [106]. This argument would be valid if all the molecules in electronic states and chemically were identical. Although, the optical emission or absorption involves electronic transitions, it must be noted that the excited state molecules do not contain the similar polarizability as the ground state molecules. A molecule in the transition between two state (ground and excited state) has indefinite

polarizability. This shows the relationship of Lorentz is applicable for any isotropic homogeneous medium which have only ground state molecules [102].

The empty cavity model was first suggested by R. J. Glauber and M. Lewenstein in 1991 [107]. Apparently, this model was used to calculate the spontaneous emission rates that are available in many publications [108-111]. Shibuya in 1983 suggested the ellipsoidal cavity shape based on virtual cavity model in preference to spherical cavity [105, 112]. However, applying the suggested model of Shibuya to molecules that absorb light yields results that contradict the electronic transitions discussed above. D. Toptygin et al. (2002), suggested the ellipsoidal cavity model equations, which involves combining the electronic transition probability with radiative decay rate and absorption cross section, thereby considering the effect of the optical properties of the local surrounding media [96, 113].

2.5 CdSe/ZnS Quantum dots as ion sensing of local surrounding media

The CdSe/ZnS based Qdots is a good candidate for various ion sensing applications. Ion sensing using Qdots can be performed through analyte induced changes in the photoluminescence spectra of Qdots. These kinds of sensors are mainly classified based on the principle of chemiluminescence and photoluminescence. On the other hand, absorbance-based sensors utilize variation in the absorbance spectra. For ion detection, the quenching in fluorescence spectra is mainly observed after interaction between the local surrounding media molecules and Qdots. Generally, Qdots based sensors are designed based on two mechanisms: photoinduced electron transfer (PET) and resonance energy transfer (RET) [114].

Studies on the ion sensing use of cadmium based Qdots for local media was first reported in 2002 when Qdots coated with thioglycerol and L-cystein were used to

detect zinc and copper in physiological buffer samples [84]. Wang et al. used CdSe/ZnS Qdots for the sensing of chloride ion (Cl^-) by measuring the Cl^- concentration in the millimolar range, which is applicable for determining intercellular Cl^- concentrations in epithelial cells [115]. Wang et al. observed that the fluorescence quenching of Qdots is caused by the adsorption of chloride ions to the conjugated water soluble CdSe/ZnS by means of electron transfer. Some studies on determining Cl^- ion concentrations considered the photoluminescence lifetime of Qdots [116]. Gauci et al. studied the hydroxide ion sensing ability of CdSe/ZnS Qdots via carboxylic acid by fluorescence quenching and they discussed these results by photoinduced electron transfer [117].

2.6 Overview of research on cavity models

Studies on the applications of water-soluble CdSe/ZnS colloidal Qdots as sensors of their local surrounding media refractive index has advanced in the last decades. Lately, the use of CdSe/ZnS colloidal Qdots for the sensing of dielectric environment is being investigated as a function of the effect of local media refractive index on the radiative (fluorescence) decay rate. For instance, Aubret et al. (2016) investigated the influence of the surrounding dielectric medium on colloidal CdSe/ZnS Qdots based on three theoretical cavity models of fluorescence decay rates as a function of the surrounding media refractive index. The study found that the virtual cavity approach is the most appropriate model for describing the empirical data for two different media (*n* of water = 1.33 and *n* of sucrose = 1.46). They further observed that the performance of single colloidal Qdots as nano-sensors for the environment are similar to the plasmonic nano-sensor for same applications [11].